Simple model for granular friction

Hisao Hayakawa
Graduate School of Human and Environmental Studies, Kyoto University, Sakyo-ku, Kyoto 606-8501, Japan
(Received 13 November 1998; revised manuscript received 2 June 1999)

We propose a simple phenomenological model to describe the motion of a plate on granular layers pushed at a constant speed. The model contains the order parameter characterizing the transition from a solidlike state to a liquidlike state. The model reproduces the hysteresis in frictional force and the universal profile of the slip velocity, which are observed in experiment. Our model predicts that the area of hysteresis loop depends on the pushing speed. [S1063-651X(99)13910-2]

PACS number(s): 81.05.Rm, 45.05.+x, 05.20.Dd, 05.70.Jk

I. INTRODUCTION

Recently, much attention has been paid to physics of granular materials. Unlike usual solids, liquids, or gases, granular materials are known to show complex dynamical behaviors [1], such as convection [2], size segregation [3], standing waves and localized excitations under vertical vibration [4], and $1/f^{4/3}$ spectra in a narrow tube [5].

Friction in granular layers is an interesting subject of fundamental physics. This subject is also important in the physics of earthquakes [6,7]. The simplest situation in which to consider granular friction is the following. Place a plate on lubricants such as granular particles and push the plate at a constant speed. When the speed is low, we can observe stick-slip motion of the plate, while at high speeds we can see a steady sliding of the plate. Similar behaviors have been observed even in atomic dry friction and and melt fractures in polymers [8,9]. Recently, Nasuno and co-workers [10] reported a sensitive measurements of frictional forces produced by granular particles in the above situation. They found that the frictional force is multi-valued and exhibits a hysteresis, whereas the frictional force is almost a constant when the slip velocity is decreased. They also reported a universal form in instantaneous velocity profile during slip in the stick-slip regime.

In this paper, we propose a simple phenomenological model to describe the physics of granular friction. The situation under consideration corresponds to the experimental situation by Nasuno and co-workers [10]. We will demonstrate that the universal form in slip velocity profile can be observed in our model, which is quite similar to the experimental one. In the limit of low driving speed, the velocity profile can be represented by an analytic function.

The organization of this paper is as follows. In the next section, we will introduce our phenomenological model and explain the physical relevancy of our model. In Sec. III, we will present the result of simulations of our model, in which we reproduce some of characteristic results of experiments. We also report some interesting new results which have not, to our knowledge, been reported in any experiments. In Sec. IV, we will discuss our results. Some of our findings can be understood by analytic consideration in the limit of low driving speed. In Sec. V, we will give concluding remarks.

II. MODEL

Our approach is inspired by the phenomenological model proposed by Carlson and Batista [11]. They assume that the friction dynamics is characterized by the coupled equations for the displacement of the plate and the order parameter that specifies the state of granular particles.

We also adopt a phenomenology which is a set of coupled equations of the displacement and the order parameter. However, our model contains two essential differences from theirs. First of all, we take into account some characteristics of the distinct element method (DEM), which is a standard method for simulating granular particles [2,12,13]. In particular, we regard Coulomb's friction law during the collision of particles as one of the key points concerning granular frictions. Namely, the shear friction between two colliding granular particles is proportional to the relative velocity for small relative velocity and is a constant which is the Coulomb's law for large relative velocity in granular collisions. Therefore, our frictional term is not proportional to the relative velocity of layers, but the friction is saturated when the relative velocity is large. This friction mechanism is thought to be important in recovering the characteristic hysteresis observed in the experiment [10]. Second, we introduce the fracture mechanism of the stress network in granular layers in our model. This idea reflects recent indications of the importance of bridging and its fractures in friction processes [14].

Here let us explain our model explicitly. Let the mass of the plate be M, and its center of mass be located at x. We assume that the friction between the granular layers and the block is characterized by the order parameter θ, where $\theta = 1$ represents a solidlike state, i.e., the grains are in contact with each other and there is a stress network in the granular layers. The plate is pushed by a driving motor with the constant speed V; the plate is connected to the motor by a Hookian spring (the spring constant k).

Thus, the equations of the block are given by

$$M\ddot{x} = k(Vt - x) - \frac{\partial}{\partial x} W - \mu M g F_{\mathrm{fr}}\left(\frac{\dot{x}}{u_0(V)} \right), \qquad (1)$$

where g and μ are, respectively, the gravitational acceleration and the dynamical friction constant. We adopt the friction force $F_{\mathrm{fr}}(x)$ as

$$F_{\rm fr}(x)=\tanh(x) \quad \text{for } x>0, \quad F_{\rm fr}(x)=bx \quad \text{for } x<0, \quad (2)$$

where we assume that b is a large constant, which essentially inhibits the motion with negative velocity. Note that the saturation of the friction in $\tanh(x)$ for large velocity corresponds to Coulomb's friction law as in the DEM model [12,13]. The potential W is given by

$$W=\frac{k\theta\xi^2}{2}\left[1-\exp\left(-\frac{(Vt-x)^2}{\xi^2}\right)\right], \quad (3)$$

which plays an important role as a resistance force in the solidlike state. We adopt here the Gaussian-Taguchi model, introduced in the simulation of fracture mechanics [15], which has the stress $-\partial W/\partial x \propto -ky\exp(-y^2/\xi^2)$ with the deflection of the spring $y=Vt-x$ from the natural length and the critical length ξ for the fracture. Namely, this model contains a resistance force that cancels the elastic force by the deflection of the spring for small $y \ll \xi$, while no resistance force exists for large $y \gg \xi$ because of fracture of the stress network. The reason we introduce a continuous fracture model is (i) to represent precursor events before main slips and (ii) to represent a state in which stress networks are partially broken. Note that in our model the static friction is not introduced explicitly but is replaced by the fracture mechanism of the stress network.

We supplement the equation of the motion of the plate with an equation for the order parameter, because a sort of phase transition between the solidlike and liquidlike states plays an important role. It is obvious, as in Eq. (3), that the stress network plays no role in a liquidlike state but plays an essential role in a solidlike state. In other words, we may regard the order parameter as the density of the stress network.

We assume that the equation of the order parameter is similar to a time dependent Ginzburg-Landau equation [16] as in the usual dynamics of phase transitions,

$$\tau\dot{\theta}=\Theta(\theta,a(\dot{x}))-\frac{\partial W}{\partial\theta}-\zeta(V)\theta\dot{x}, \quad (4)$$

where τ is a characteristic time scale. The first term $\Theta(\theta,a)\equiv\theta(\theta-a(\dot{x}))(1-\theta)$ on the right hand side of Eq. (4) characterizes the dynamics of the ''liquid-solid transition,'' where θ increases (decreases) when $\Theta>0$ $(\Theta<0)$. The point at which $\Theta=0$ is satisfied is a fixed point. When Θ is a decreasing function of θ and changes its sign at a fixed point, the fixed point is stable. In other cases, e.g. a double root point of $\Theta=0$, or where Θ is an increasing function of θ at a fixed point, the fixed points are unstable. In Eq. (4), $a(\dot{x})$ is assumed to be a function of sliding velocity, where we adopt $a(\dot{x})=\tanh^2(\dot{x}/v_0)$ with a characteristic velocity v_0 to satisfy the following properties. When there is no sliding, the system should be in a solid state. Thus, Θ has a stable fixed point at $\theta=1$ corresponding to the solid state and $\theta=0$ is the double root of $\Theta=0$ when the velocity is zero. The system should be in a liquid state when the sliding velocity is infinite. Thus, we assume that $\theta=1$ becomes the double root of $\Theta=0$ and a stable fixed point exists at $\theta=0$, corresponding to the liquid state, when the velocity is infinite. For finite velocity, both (liquid and solid) states become locally stable, and $\theta=a(\dot{x})$ is an unstable fixed point. The last term in Eq. (4) represents the shear-induced melting force, which is the same form introduced by Carlson and Batista in [11].

We make two remarks on our modeling. First, the model by Carlson and Batista [11] in which they adopt $\Theta=\theta(1-\theta)$ and the liquid state and the solid state are always an unstable fixed point and a stable fixed point, respectively, may be inadequate to describe the dynamics of phase transitions. Second, we expect that the behavior is not sensitive to the choice of W and Θ, as in the case of conventional phase transitions.

III. SIMULATION

Let us analyze our model. At the first stage we nondimensionalize the model. The variables in the unit of space, time, and velocity are respectively scaled by Mg/k, $\sqrt{M/k}$, and $g\sqrt{M/k}$. Thus, the dimensionless equations corresponding to Eqs. (1), (3), and (4) are given by

$$\frac{d^2}{d\hat{t}^2}\hat{x}=\hat{V}\hat{t}-\hat{x}-\frac{\partial\hat{W}}{\partial\hat{x}}-\mu F_{\rm fr}\left(\frac{d\hat{x}/d\hat{t}}{\hat{u}_0(\hat{V})}\right), \quad (5)$$

$$\hat{W}=\frac{\theta\hat{\xi}^2}{2}\left[1-\exp\left(-\frac{(\hat{V}\hat{t}-\hat{x})^2}{\hat{\xi}^2}\right)\right], \quad (6)$$

$$\hat{\tau}\frac{d}{d\hat{t}}\theta=\Theta\left(\theta,a\left(\frac{d\hat{x}}{d\hat{t}}\right)\right)-\frac{\partial\hat{W}}{\partial\theta}-\hat{\zeta}(V)\theta\frac{d\hat{x}}{d\hat{t}}. \quad (7)$$

We restrict our interest to the case of $k=135$ N m^{-1}, $M=1.1\times10^{-2}$ kg, $g=9.8$ m/s^2, and $\mu=0.45$. All of these parameters correspond to the typical setup of the experiment by Nasuno and co-workers [10]. Thus, the unit length, the unit time, and the unit speed in the dimension-less unit are about $Mg/k=0.8$ mm, $\sqrt{M/k}=9.0\times10^{-3}$ sec, $g\sqrt{M/k}=9$ cm/sec in the actual scale. To achieve the stick-slip motion in the very low velocity V region, we introduce the V dependence as $\hat{\zeta}(V)=\zeta_0/\tanh(V)$ and $\hat{u}_0(V)=\bar{u}\tanh(V)$, with $\zeta_0=\bar{u}=0.1$ in the dimensionless unit. Our choice of $\hat{\zeta}(V)$ and $\hat{u}_0(V)$ corresponds to the nonexistence of a characteristic velocities in the low V limit because $\zeta^{-1}(V)$ and $u_0(V)$ can be characteristic velocities in the transition from stick-slip motion to creep if they are constants. The critical length $\hat{\xi}$ in Eq. (6) and the time scale $\hat{\tau}$ in Eq. (7) are assumed to be 0.7 and 3.0×10^{-2}, respectively. Note that the critical length $\hat{\xi}$ determines the static friction, because the stress network exists for $\hat{V}\hat{t}-\hat{x}<\hat{\xi}$, while it disappears for $\hat{V}\hat{t}-\hat{x}>\hat{\xi}$. Therefore, the choice of $\hat{\xi}=0.7$ is from our expectation that the static friction constant is close to 0.7. On the other hand, we choose small $\hat{\tau}$, because we may expect that the time scale of phase change between liquids and solids is much shorter than the time scale for the oscillation of springs. The dimensionless parameters v_0 in $a(\dot{z})$ in Eq. (4) and b in Eq. (2) are set to be $\hat{v}_0=v_0/(g\sqrt{M/k})=1.0$ and $\hat{b}=bMg/k=10^4$, respec-

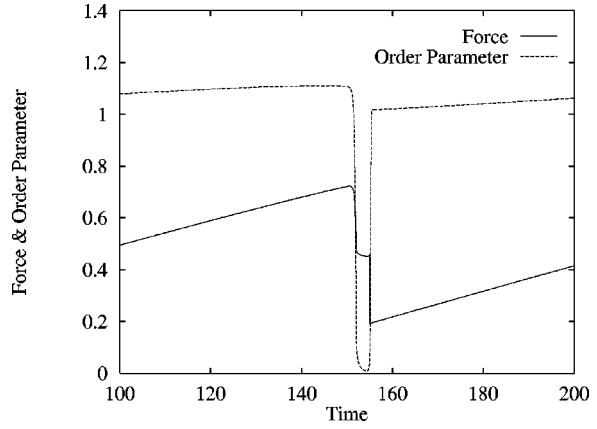

FIG. 1. A typical time evolution of dimensionless frictional force $d^2\hat{x}/d\hat{t}^2-(\hat{V}\hat{t}-\hat{x})$ and the order parameter θ during a slip event around $\hat{t}=150$. We show the data in the first slip for $\hat{V}=5\times10^{-3}$.

tively. We adopt the classical fourth order Runge-Kutta method for numerical integration with the time interval $\Delta\hat{t}=10^{-5}$.

At first we simulate the model for relatively low $\hat{V}$, where typical stick-slip motion of the block can be observed. Figure 1 shows typical behavior of a dimensionless frictional force defined by $(d^2\hat{x}/d\hat{t}^2)-\hat{V}\hat{t}+\hat{x}$ and θ during a slip event. The order parameter is a little larger than its stable value 1 before/after the slip. During the phase change from the solid state to the liquid state, the frictional force (and deflection) is quickly reduced because the stress network has been broken.

In Fig. 2, we plot the profile of slip velocity, where $\hat{t}=0$ is fixed at the end of slip events. All the data between $\hat{V}=2.5\times10^{-4}$ and 2.5×10^{-3} seem to be on a universal curve as in the experiment. Although we can observe stick-slip motion for larger V, the profile depends on $\hat{V}$ in such regions. Even in the universal region, we can find a nonuniversal part of the profile near the start of slip, where the velocity is greater for large $\hat{V}$ value than for small $\hat{V}$.

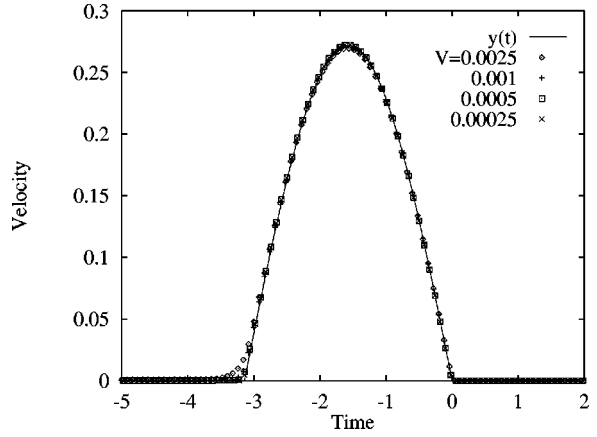

FIG. 2. Instantaneous dimensionless velocity $d\hat{x}/d\hat{t}$ as a function of dimensionless time $\hat{t}$ during slip in the stick-slip regime. The origins of the pulses are forced to agree at the end of each event. The solid curve is $-0.272\sin(\hat{t})$ which is obtained by the classical Amontons-Coulomb's law.

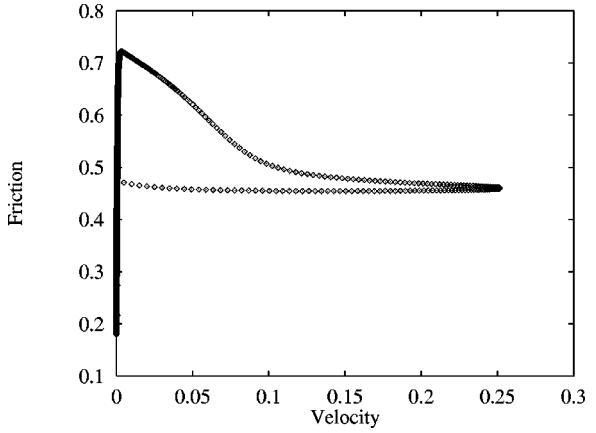

FIG. 3. The hysteresis loop of the friction force $d^2\hat{x}/d\hat{t}^2-(\hat{V}\hat{t}-\hat{x})$ in dimensionless unit as a function of dimensionless slip velocity $d\hat{x}/d\hat{t}$ for driving speed $\hat{V}=0.01$.

In Fig. 3, we plot the dimensionless frictional force $(d^2/d\hat{t}^2)\hat{x}-\hat{V}\hat{t}-\hat{x}$ as a function of slip velocity $\hat{V}$. As in Fig. 3 we obtain a hysteresis loop for the friction which is similar to that observed in the experiment. Hysteresis loops, however, depend on $\hat{V}$ in our model. In our simulation, the area of the hysteresis becomes narrower, when the driving velocity becomes slower. To check quantitative behavior of the area of hysteresis loop $S(\hat{V})$ as a function of $\hat{V}$, we evaluated the area of the loop for each $\hat{V}$ as follows. First, we distinguish the data for $d\hat{x}/d\hat{t}>10^{-3}$ from others. For one loop, we evaluated the area of the loop S by reducing the area of the upper branch S_u defined through the time derivative of the frictional force $(d/d\hat{t})f_i>0$ and enlarging that of the lower branch S_l defined by $(d/d\hat{t})f_i<0$, $S=S_u-S_l$, based on trapezoid's rule as $S_m=\Sigma_i(f_i+f_{i+1})|v_{i+1}-v_i|/2$, where $m=u$ or l, and f_i and v_i are, respectively, the frictional force and the velocity of the ith data in dimensionless units. The data between $\hat{V}=2.5\times10^{-4}$ and 1.0×10^{-2} can be fitted by a power law (see Fig. 4)

$$S\simeq c\hat{V}^{\alpha},\quad c=0.248,\quad \alpha=0.547\pm0.033. \tag{8}$$

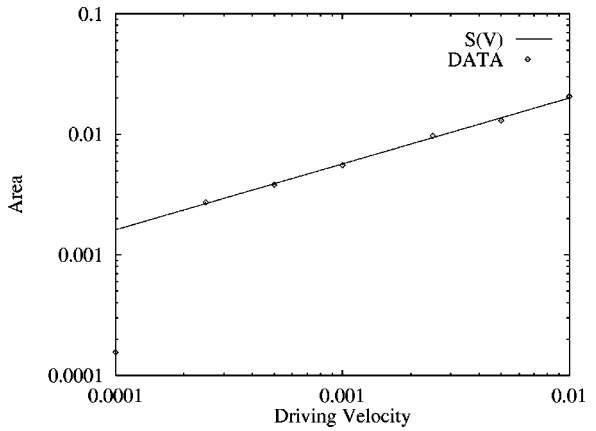

FIG. 4. Log-log plot of the dimensionless area $S(\hat{V})$ of the hysteresis loop evaluated from Fig. 3 as a function of driving velocity $\hat{V}$. The solid line represents $S(\hat{V})=0.248\hat{V}^{0.547}$.

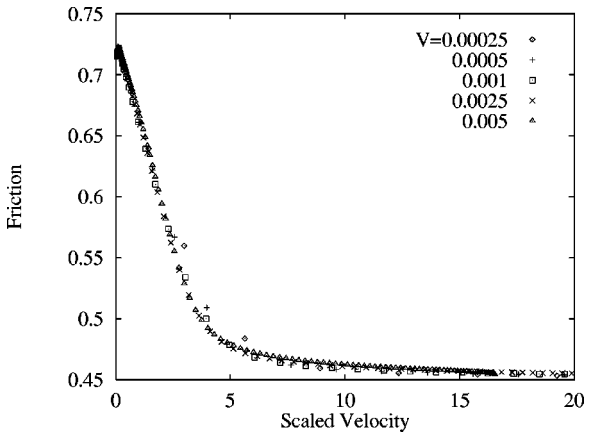

FIG. 5. The friction force in a upper branch ($d\hat{x}/d\hat{t}>0.3$ and the force decreases with time) as a function of scaled velocity $(d\hat{x}/d\hat{t})/\hat{V}^{0.78}$.

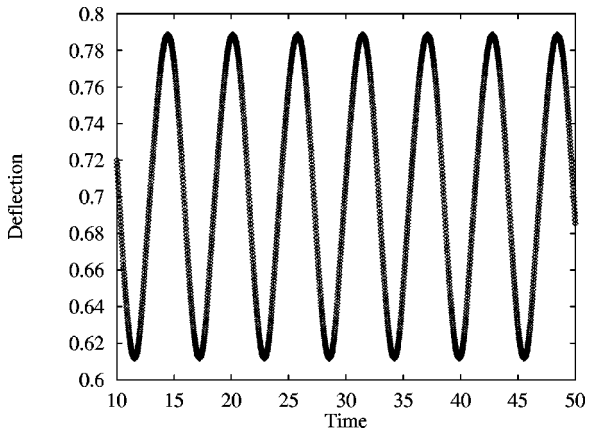

FIG. 6. The oscillation in deflection $\hat{V}\hat{t}-\hat{x}$ as a function of time $\hat{t}$ for $\hat{V}=0.1$.

Thus, the area may become zero in the low velocity limit, which means that the transition from the static friction state to the dynamic friction state is instantaneous as in the classical Amontons-Coulomb law. The result in Eq. (8) is an interesting one which to our knowledge has not been reported in experiments. We are not sure whether the actual experiments reproduce such a power law or how this law is structurally stable. This result should be checked by experiments and direct simulation based on DEM to verify the validity of our picture. At present we do not know how to produce such a power law. We also found that the force f_i in the upper branch of the loop defined above obeys

$$f_i=F(\dot{x}/V^{\beta});\quad \beta\simeq 0.78, \tag{9}$$

where $F(x)$ is a universal function (Fig. 5). Since the exponent β is different from α, we believe that the power law in Eq. (8) comes from complicated combinations of several processes.

IV. DISCUSSION

Our model may reduce to the classical Amontons-Coulomb model in the limit of $V\to 0$, which can be analyzed by elementary mechanics. The elementary analysis can be outlined as follows. The plate is stationary for $y=Vt-x<y_1\equiv\mu_s Mg/k$ from the natural length, where μ_s is the static friction constant. The slip motion of the block is nondissipative, and it conserves the energy $E=\frac{1}{2}M(v-V)^2+(k/2)(y-y_2)^2$, where equilibrium position y_2 is given by $\mu Mg/k$. The trajectory in the phase space (y,v) is a semicircle whose center is at (y_2,V) and its radius is given by $\sqrt{V^2+(k/M)(y_1-y_2)^2}$. The plate stops when y becomes $2y_2-y_1$, and the plate is at rest during $2(y_1-y_2)/V$. Thus, one period from the beginning of one slip to the beginning of the next slip is given by

$$T=2\left\{\pi-\sin^{-1}\left(\frac{y_1-y_2}{\sqrt{MV^2/k+(y_1-y_2)^2}}\right)\right\}\times\sqrt{M/k}+2(y_1-y_2)/V.$$

The time dependence of velocity $\dot{x}$ is represented by a positive part of the sinusoidal curve whose amplitude is $\sqrt{M/k}(\mu_s-\mu)g$ in the low V limit, which satisfies $V^2\ll k(y_1-y_2)^2/m=mg^2(\mu_s-\mu)/k$.

The results in the area of the hysteresis curve are indirect evidence that our model is reduced to the Amontons-Coulomb model. Thus, we try to compare our data on slip velocity with that by the Amontons-Coulomb law. The solid line in Fig. 1 is the theoretical prediction $(d/d\hat{t})\hat{x}(\hat{t})=-A\sin(\hat{t})H(d\hat{x}/d\hat{t})$ with $A=0.272$ in the slow $\hat{V}$ limit, where $H(x)=1$ for $x\geqslant 0$ and $H(x)=0$ for otherwise. Note that the amplitude of the slip velocity is $(y_1-y_2)\sqrt{M/k}$ in the Amontons-Coulomb limit $(V\to 0)$. Thus, the dimensionless amplitude is deduced to be $\mu_s-\mu$. The static friction constant may be evaluated by $\hat{\xi}=0.7$, and $\mu=0.45$. Thus we expect that the dimensionless amplitude is close to 0.25. In other words, the static friction constant evaluated from our simulation is 0.72, which is a little larger than $\hat{\xi}=0.7$. Thus, the universal behavior in low V is thought to be the state in which the inertia of spring motion can be neglected.

The results reported here are consistent with experimental results on stick-slip motion [10]. For example, we need the condition $V^2\ll mg^2(\mu_s-\mu)/k$ in order to reach the universal law governing the velocity profile of slip. In Ref. [10] the universal law is satisfied below $V=1137.27\mu$ m/s for $k=135$ N/m. We, thus, obtain $V^2k/[mg^2(\mu_s-\mu)]\simeq 0.083$, where we estimated $\mu_s=0.65$ and $\mu=0.45$ from experimental data. Therefore, the universal behavior of the slip is only observable in the slow velocity region as in our model simulation. Note that we can observe a little asymmetric velocity profile of slip in the actual experiment [10]. We believe that this asymmetric behavior can be understood by the occurrence of creep motion before the main slip. In fact, even in our simulation, we can observe a small asymmetry in the profile, where the velocity before the main slip is larger than that after the main event.

This model obviously describes the transition from the stick-slip motion to a periodic oscillation (see Fig. 6). Unfortunately, however, this model is not appropriate to describe a steady sliding motion. To describe the transition from the periodic motion to the steady sliding motion we may need to replace Eq. (1) by, e.g.,

$$M\ddot{x}=k(Vt-x)-\frac{\partial}{\partial x}W-\mu MgF_{\mathrm{fr}}\left(\frac{\dot{x}}{u_0(V)}\right)-M\gamma\dot{x}, \tag{10}$$

where γ should be small for consistency with the result for small V. The existence of such a friction term ensures relaxation to a steady sliding motion. We should not be surprised by the existence of the term proportional to $\dot{x}$, because the collective motion of granular particles inside layers is complicated and crucial under the high shear rate. However, we will not discuss the details of this model because at present the connection between collective motion of grains and the term $\gamma\dot{x}$ is not clear.

Our result reported here may crucially depend on our choice of $\zeta(V)$ and $u_0(V)$. If we change $\zeta(V)$ and $u_0(V)$ as constants, we observe creep motion in the low V limit, but V dependence on hysteresis disappears. Our model cannot predict the change of spatial structure during slips, nor can it predict the order parameter. To clarify unclear points and check the results reported here, we need to carry out DEM simulation, which is now in progress. The result of our DEM simulation will be reported elsewhere.

V. CONCLUSION

In conclusion, we propose a simple phenomenological model for granular friction. Our model reproduces some characteristic results observed by Nasuno and co-workers [10] in stick-slip motion, such as the universal velocity profile in the slip and hysteresis loops. Our model shows that the area of hysteresis loop S depends on the driving velocity as $S\sim V^{0.547}$. Our model also can describe the transition to an oscillating region as the driving velocity increases, but is not appropriate for describing of steady sliding motion.

ACKNOWLEDGMENTS

The author thanks S. Sasa and S. Nasuno for their useful comments. This work was partially supported by the Grant-in-Aid for Science Research Fund from the Ministry of Education, Science and Culture (Grant Nos. 09740314 and 11740228).

[1] H. M. Jaeger, S. R. Nagel, and R. P. Behringer, Rev. Mod. Phys. **68**, 1259 (1996).
[2] Y-h. Taguchi, Phys. Rev. Lett. **69**, 1367 (1992); K. M. Aoki, T. Akiyama, Y. Maki, and T. Watanabe, Phys. Rev. E **54**, 874 (1996).
[3] A. Rosato, K. J. Strandburg, F. Prinz, and R. H. Swendsen, Phys. Rev. Lett. **58**, 1038 (1987).
[4] F. Melo, P. B. Umbanhowar, and H. L. Swinney, Phys. Rev. Lett. **75**, 3838 (1995); P. B. Umbanhowar, F. Melo, and H. L. Swinney, Nature (London) **382**, 793 (1996).
[5] G. Peng and H. J. Herrmann, Phys. Rev. E **49**, R1796 (1994); O. Moriyama, N. Kuroiwa, M. Matsushita, and H. Hayakawa, Phys. Rev. Lett. **80**, 2833 (1998); H. Hayakawa and K. Nakanishi, Suppl. Prog. Theor. Phys. **130**, 57 (1998).
[6] B. N. J. Perrson, *Sliding Friction: Physical Principle and Applications* (Springer, Berlin, 1998).
[7] C. H. Scholz, Nature (London) **391**, 37 (1998).
[8] See, e.g., F. Heslot, T. Baumberger, B. Perrin, B. Caroli, and C. Caroli, Phys. Rev. E **49**, 4973 (1994).
[9] A. Subbotin, A. Semenov, and M. Doi, Phys. Rev. E **56**, 623 (1997); K. Sato and A. Toda, J. Phys. Soc. Jpn. **68**, 75 (1999).
[10] S. Nasuno, A. Kudrolli, and J. P. Gollub, Phys. Rev. Lett. **79**, 949 (1997); S. Nasuno, A. Kudrolli, A. Bak, and J. P. Gollub, Phys. Rev. E **58**, 2161 (1998).
[11] J. M. Carlson and A. A. Batista, Phys. Rev. E **53**, 4153 (1996); A. A. Batista and J. M. Carlson, *ibid.* **57**, 4986 (1998).
[12] P. A. Cundall and O. D. L. Stark, Geotechnique **29**, 47 (1979).
[13] P. A. Thompson and G. S. Grest, Phys. Rev. Lett. **67**, 1751 (1991).
[14] M. E. Cates, J. P. Wittmer, J.-P. Bouchard, and P. Claudin, Phys. Rev. Lett. **81**, 1841 (1998) and references therein; P. Hebraud and F. Lequeux, *ibid.* **81**, 2934 (1998); V. Zaloj, M. Urbakh, and J. Klafter, *ibid.* **81**, 1227 (1998).
[15] Y-h. Taguchi, Mod. Phys. Lett. B **8**, 1335 (1994) [see, e.g., Eq. (2) and Fig. 1(a)].
[16] See, e.g., M. C. Cross and P. C. Hohenberg, Rev. Mod. Phys. **65**, 851 (1993).